2021

Numerical Investigation of Two-stage Vapor Compression System with Simultaneous Vapor and Liquid Injection

Ransisi Huang
University of Maryland, cchuang5@terpmail.umd.edu

Jiazhen Ling
University of Maryland

Vikrant Aute
University of Maryland

Leping Zhang
Danfoss Commercial Compressor

Numerical Investigation of Two-stage Vapor Compression System with Simultaneous Vapor and Liquid Injection

Ransisi HUANG[1,3], Jiazhen LING[1], Vikrant AUTE[1]*, Leping ZHANG[2]

[1]Department of Mechanical Engineering, University of Maryland,
College Park, Maryland, United States

[2]Danfoss Commercial Compressor,
Beijing, China

[3]Building Technologies and Science Center, National Renewable Energy Lab,
Golden, Colorado, United States

* Corresponding Author: vikrant@umd.edu

ABSTRACT

Two-stage vapor compression systems can be advantageous over single-stage systems by providing improved system performance, lower discharge temperature and reduced throttling losses. These systems employ various intermediate configurations, such as liquid injection and vapor injection. This paper presents a configuration for a R1234ze(E) two-stage air-conditioning system using a turbo compressor with two injection ports, one for vapor injection and the second for liquid injection. The liquid injection is used to cool the motor and electronics. A component-based representation and solution approach was used to simulate the two-stage compression system with simultaneous vapor and liquid injection at steady state. The turbo compressor was represented using a customized performance map. The condenser and the evaporator were modeled using finite-volume approach. A parametric study was conducted to assess the impact of the following three variables on the system performance: vapor injection ratio, condenser air flow rate, and discharge pipe pressure drop. The simulation results show that as the vapor injection ratio increased, the system performance undergoes a tradeoff between an enhanced subcooling effect (and thus enhanced unit refrigeration capacity) and a decreased suction mass flow rate. Maximum COP occurs when the vapor injection ratio was 0.1. The results also show that as the condenser air flow rate increased, both the capacity and power consumption (including fan power) increased monotonically, and COP increased first and then decreased. At 75% load, the COP improvement at the optimum flow rate was marginally less than 0.5%. Lastly, higher discharge pipe pressure drop increased the discharge pressure. It showed very small effect on the overall system performance at the condition selected for the current study.

Keywords: two-stage compression system, turbo compressor, multi-port injection, motor cooling, component-based steady-state simulation

1. INTRODUCTION

Improving the performance of vapor compression air conditioning systems is one of the measures to alleviate the energy consumption and environmental impact associated with these systems. Operation of such systems with a large difference between the condensing and evaporating temperature will result in deteriorated capacities, and declining COP. Moreover, the rising compression ratio may lead to an extremely high discharge temperature and consequently a shut down.

An effective approach to handle these challenges is to use two-stage vapor compression systems. These systems may employ various intermediate configurations for performance and operation range enhancement, such as liquid injection (or direct injection), flash tank vapor injection, economizer vapor injection, ejector injection, etc. Heo, et al. (2011) revealed that the use of vapor injection could significantly enhance the heating capacities. Aikins, et al. (2013) reviewed various two-stage compression heat pump systems, and reported that the capacity and COP of these two-stage cycles could be enhanced by up to 30% compared to single-stage cycles. Qi, et al. (2017) proposed a hybrid

vapor injection cycle with a two-phase ejector. The simulation results indicated that COP of the hybrid system could be increased by 1.1% to 3.3% compared to the economizer and flash tank vapor injection cycle.

In terms of the modeling of the two-stage systems, Torrella, et al. (2011) proposed a general analysis methodology that could handle 6 configurations of two-stage vapor compression systems. They also established a generic COP expression based on the subcooling parameter and desuperheating parameter. Jiang, et al. (2015) extended Torrela's method to a more general model for two-stage compression systems, and in a later publication (Jiang, et al. 2016), they applied the general model to investigate the effect of different parameters on the optimum injection pressure.

We identified two research gaps from the current research work related to two-stage compression systems. First, the compressor in these systems was commonly rotary compressor (scroll compressor in particular), and most of these systems were geared toward small/medium capacity designs. The investigation of large-scale two-stage compression systems with turbo compressor was very limited. Secondly, the modeling approach of the two-stage systems was dominantly thermodynamic models. The use of component-based simulation architecture with finite-volume HX models for two-stage system analysis was also limited.

Therefore, this study presents a two-stage vapor compression system with a turbo compressor for large capacity application, with R1234ze(E) being the refrigerant. The turbo compressor has a liquid injection port and a vapor injection port. The liquid injection serves to cool down the motor and electronics. To simulate the two-stage system with simultaneous vapor and liquid injection, we used a component-based representation and solution approach. A parametric study was conducted to assess the impact of vapor injection ratio, condenser air flow rate, and discharge pipe pressure drop on the system performance.

2. SYSTEM MODELING APPROACH

2.1 System description

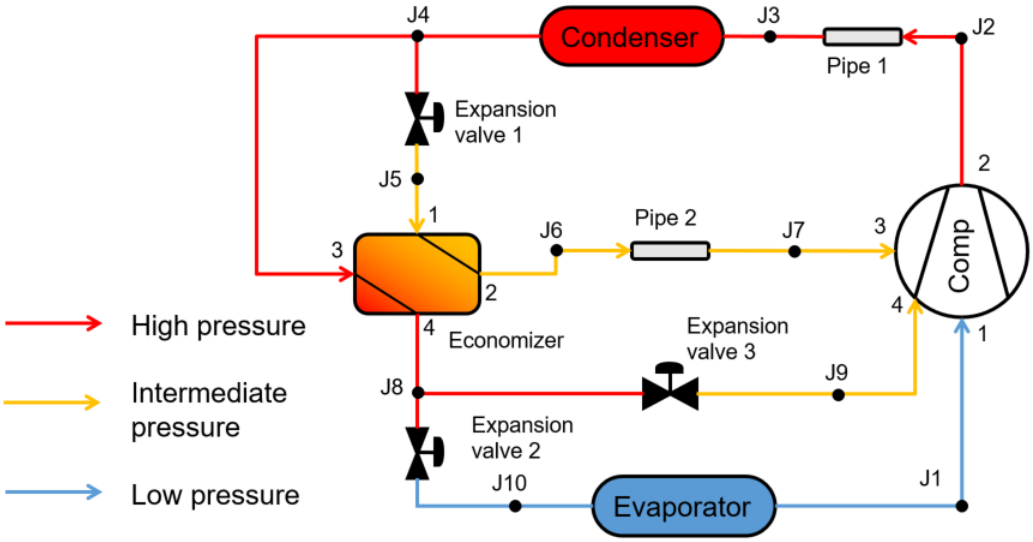

Figure 1: Schematic of simultaneous vapor and liquid injection system

Figure 1 shows the system configuration. The condenser and evaporator are microchannel air-to-refrigerant HXs. The economizer is a fluid-to-fluid HX. Port 1 and 2 of the economizer is the cold fluid end, while port 3 and 4 the hot fluid. The compressor is a turbo compressor with two injection ports. Port 3 is for vapor injection, and port 4 is for liquid injection. The vapor injection is enabled by expansion valve 1 and the economizer. The vapor injection ratio of the system is given by

$$R_{vi} = \frac{\dot{m}_{valv1}}{\dot{m}_{cond}} = \frac{\dot{m}_{comp,3}}{\dot{m}_{comp,2}} \tag{1}$$

where $\dot{m}_{valv1}$ is the mass flow rate of the expansion valve 1. The liquid injection through port 4 is for compressor motor cooling. The subcooled liquid from the economizer port 4 is expanded by expansion valve 3 before being

injected into the turbo compressor. This stream of refrigerant is used for cooling the motor and electronics. The motor cooling liquid injection ratio is given by

$$R_{li} = \frac{\dot{m}_{comp,4}}{\dot{m}_{comp,1}} = \frac{\dot{m}_{valv3}}{\dot{m}_{eco,4}} \tag{2}$$

where $\dot{m}_{eco,4}$ is the mass flow rate of the economizer port 4. Pipe 1 and pipe 2 in the system are the discharge pipe and the injection pipe, respectively.

The system refrigerant is R1234ze(E). The turbo compressor was represented with a customized performance map. The condenser and evaporator were simulated using an in-house finite volume air-to-refrigerant heat exchanger model (Jiang, et al. (2006)). The model adopts a network viewpoint allowing for arbitrary tube circuitry and mal-distribution of fluid inside the tube circuits. It implements a segment-by-segment approach within each tube to account for refrigerant flow pattern through the tube as well as air distribution across the heat exchanger. The economizer model was a lumped-effectiveness model.

2.2 Component model and system solution approach

We used a steady-state component-based simulation framework for vapor compression systems to simulate the simultaneous vapor and liquid injection system. The system was represented as a network of black-box components with either pressure or mass flow boundary condition (Table 1). It should be noted that the three expansion valves, although they are categorized as the pressure-based components, were all bypassed in the simulation.

Table 1: Component model boundary condition type

Boundary condition type	Component	Component model inputs	Component model outputs
Mass flow based	Condenser, evaporator, economizer, tube	$(P, h, \dot{m})_{\text{inlet ports}}$	$(P, h)_{\text{outlet ports}}$
Pressure based	Compressor, expansion valve	$(P, h)_{\text{inlet ports}}$, $(P)_{\text{outlet ports}}$	$\dot{m}_{\text{all ports}}$, $(h)_{\text{outlet ports}}$

The assumptions/simplifications for the system simulations are as follows:

- All three expansion valves are bypassed (represented with an isenthalpic process without detailed modeling).
- The pressure levels at the two injection ports of the compressor (3 & 4) are equal.
- The motor cooling liquid injection ratio of the compressor is a constant parameter.
- The economizer model has a constant effectiveness of 0.93, and does not account for pressure drop.

Given these, we formulated a system of equations that describe the steady state of the system, based on continuity, energy balance, and momentum balance of each junction. The equations mentioned here does not involve any component-level equations that govern the heat transfer, hydraulic relations and thermodynamics in the components. And then we determined the component execution order in such a way that would eliminate the most variables and the equations. The reduced system of equations is shown in Table 2. As is shown, we need 3 additional design criteria to close the equations. They will be specified in 2.3. The equations were solved using Broyden's method (Dennis & Schnabel, 1996) to obtain the steady-state solution of the system.

Table 2: Non-linear residual equation formulation

No.	Unknown variable	Residual equation	Comment
1	$P_{comp,1}$	$(\dot{m}h)_{comp,1} = (\dot{m}h)_{evap,out}$	Energy balance at J1 (Figure 1)
2	$P_{comp,2}$	$(\dot{m}h)_{comp,3} = (\dot{m}h)_{pipe2,out}$	Energy balance at J7
3	$P_{comp,3}$ (= $P_{comp,4}$ = $P_{eco,1}$)	$(\dot{m}h)_{comp,4} = (\dot{m}h)_{valve3,out}$	Energy balance at J9
4	$h_{comp,1}$	$P_{evap,out} = P_{comp,1}$	Pressure balance at J1
5	$h_{comp,3}$	Convergence criterion 1	
6	$h_{comp,4}$	Convergence criterion 2	
7	$P_{valv2,\ out}$	Convergence criterion 3	

2.3 Simulations

Table 3 shows the parametric variable, the parametric range, and the test condition of the 3 simulation tests. The condenser air flow rates in the table are given in the normalized values against the minimum value. The test conditions follow the AHRI standard, and the air temperatures of each condition are shown in Table 4. The 3 convergence criteria were compressor suction SH = 2 K, condenser outlet SC = 3.36 K, and vapor injection ratio (R_{vi}). R_{vi} was set to 0.09 for test No.3 and test No.2, 100% load.

No steady state solution was found for test No.2, the 75% load case, because the subcooled liquid from the condenser could not bring the vapor injection stream to vapor phase regardless of the value of R_{vi}. Therefore, we added 1000 W of heat to the injection pipe (pipe 2), and also accounted for it in the COP calculation. Also, for this particular test, we changed the convergence criterion from R_{vi} to injection SH = 1 K. For all simulation tests, the motor cooling liquid injection ratio (R_{li}) was set to 0.01.

Table 3: Summary of the simulation tests

Test No.	Test condition	Parametric variable	Range	Others
1	100% load	Vapor injection ratio	0.06 – 0.11	SH_{suc} = 2 K, SC = 3.36 K
2	100% load	Normalized condenser air flow rate	1 – 1.5	SH_{suc} = 2 K, SC = 3.36 K, R_{vi} = 0.09
	75% load		1 – 1.5	1000 W applied to injection pipe; SH_{suc} = 2 K, SC = 3.36 K, SH_{inj} =1 K
3	100% load	Discharge pipe pressure drop	7 – 19 kPa	SH_{suc} = 2 K, SC = 3.36 K, R_{vi} = 0.09

Table 4: 100 and 75 percent load condition (AHRI340/360)

Load condition	Indoor air		Outdoor
	T_{db} (K)	T_{wb} (K)	T_{db} (K)
100%	299.82	292.59	308.15
75%	299.82	292.59	300.65

3. RESULTS AND DISCUSSION

3.1 Effect of vapor injection ratio

As shown in Figure 2 (a), as R_{vi}, increases, capacity first increases and then decreases, while power consumption presents the opposite trend. As a result, the maximum COP occurs when R_{vi} = 0.1. To illustrate the effect of R_{vi} on Q, Figure 3 compares the system P-h diagram at R_{vi} = 0.06, R_{vi} = 0.1 (the optimum injection ratio), and R_{vi} = 0.11. *JX* (X = 1,2…) represents the junction number in Figure 1. Increasing R_{vi} from 0.06 to 0.1 resulted in an enhanced subcooling effect of the economizer, and thus a smaller quality at the evaporator inlet (J10). This increased unit refrigeration capacity dominated the overall system capacity, despite the fact that an increased R_{vi} also led to a smaller mass flow rate in the evaporator (or suction mass flow rate). The decrease in suction mass flow rate with increasing R_{vi} is indicated in Figure 2 (b). A further increase of R_{vi} to 0.11 hardly affected the location of J8, and meanwhile moved J7 from the vapor phase into the two-phase region. This indicates that the subcooling effect of the economizer has plateaued, and therefore could no longer overcome the impact of the decreasing mass flow rate in the evaporator. Therefore, the system capacity decreased. The decrease in the injection quality at R_{vi} = 0.11 was also responsible for the increase in the compressor power consumption.

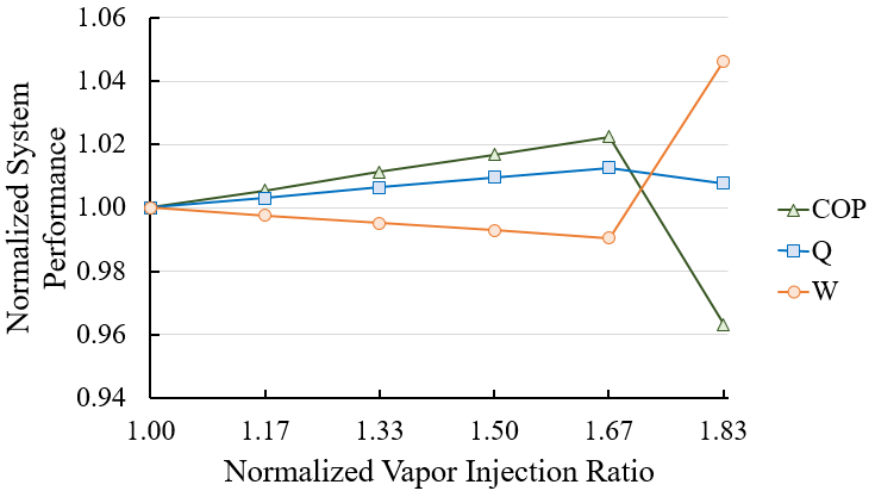

(a)

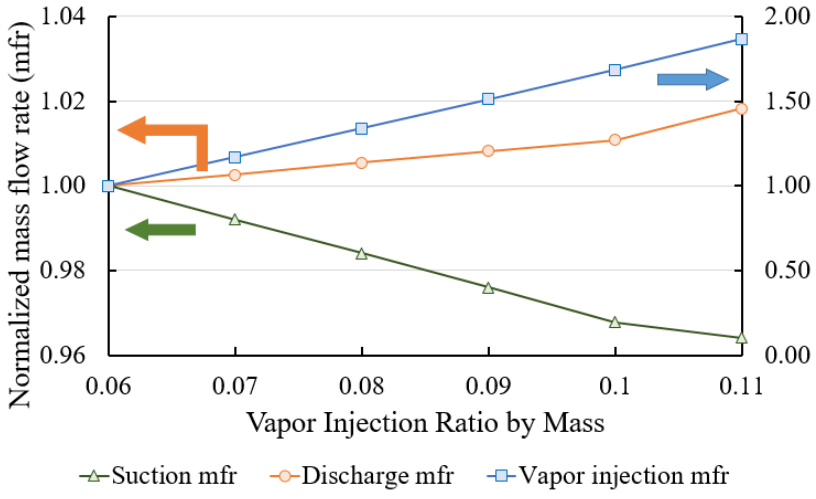

(b)

Figure 2: Effect of vapor injection ratio on (a): COP, capacity, and power consumption; (b): mass flow rates

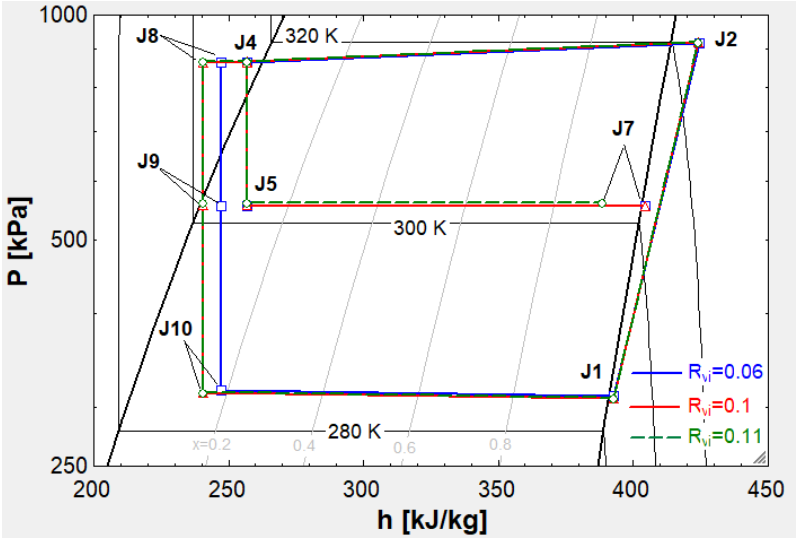

Figure 3: P-h diagrams at 3 vapor injection ratios (R_{vi})

It should be noted that the optimum R_{vi} =0.1 was obtained under the assumption of constant economizer effectiveness. In reality, the economizer effectiveness might differ depending on the operating conditions. Therefore, the optimum R_{vi} would largely depend on the performance of the economizer.

3.2 Effect of condenser air flow rate

Figure 4 (a) shows the effect of condenser air flow rate on COP, capacity, and power consumption at 100% load condition (308.15 K ambient temperature). Two sets of results are presented: the dash lines show the fan power excluded results, while the solid lines include the fan power consumption. The fan power was estimated with

$$W_{fan} = \frac{\Delta P_{air} \dot{V}_{air}}{\eta_{fan}} \tag{3}$$

where ΔP_{air} is the HX air-side pressure drop, $\dot{V}_{air}$ is the volumetric air flow rate of condenser, and η is the efficiency which was assumed to be 0.75.

As the flow rate increases, the system capacity increases monotonically. This increase was caused by two factors. The first is the slight increase in suction mass flow rate, as shown in Table 5. The second is the decreased quality at the evaporator inlet. Figure 4 (a) shows the P-h diagram of 100% load condition at 3 different flow rates. The P-h diagram shows that an increase in the flow rate leads a decreasing condensing pressure. This is because higher flow rate resulted in better heat transfer, and thus smaller approach temperature in the HX. As a result, the evaporator inlet was pushed toward a lower quality, as shown in the J10 zoom in the figure.

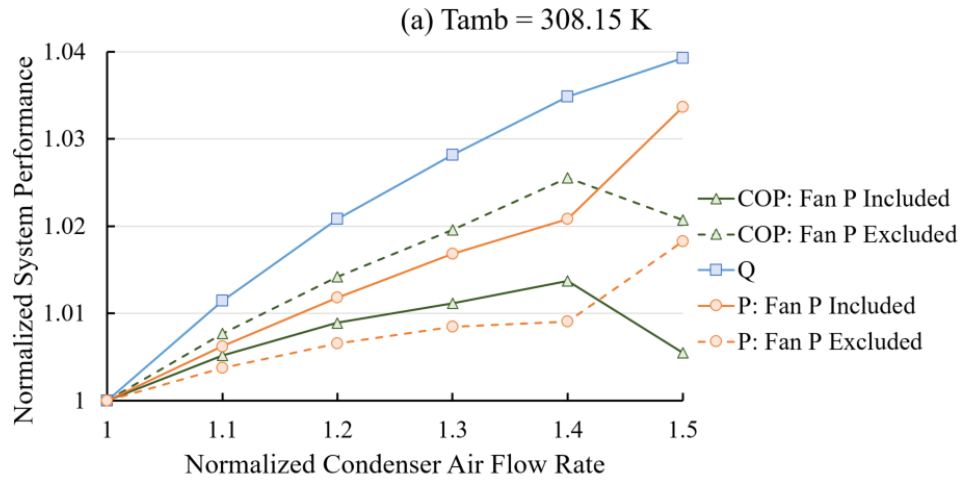

(a)

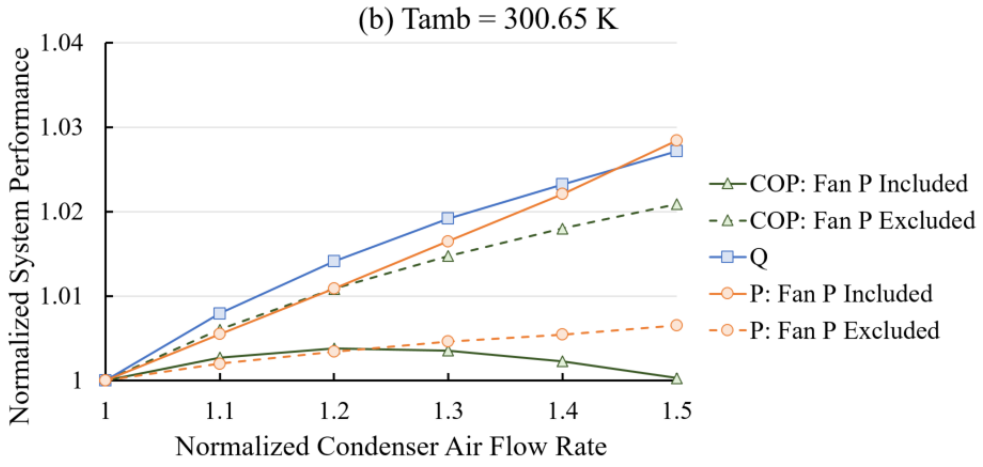

(b)

Figure 4: Effect of condenser air flow rate on system performance at (a) 100% load, (b) 75% load condition

As the flow rate increases, the power consumption (with and without fan) also increases monotonically. However, when the rate flow was increased by 50% ($\hat{V}$ = 1.5), the increase in power consumption was more dramatic than that at other flow rates. This was seen in both the compressor power and the total power, suggesting this behavior was mainly caused by compressor. The reason for this behavior is that, as the flow rate was increased by 50%, the quality at the injection point (J7) moved from vapor phase to two phase, as shown in J7 zoom in Figure 5 (a). This increase in power consumption was more significant than the increase in capacity. Therefore, system COP (with and without the fan power) started to drop when the normalized flow rate exceeded 1.4.

Table 5: Effect of condenser air flow rate on the mass flow rates (normalized)

$\hat{V}$ (-)	100% load		75% load	
	Normalized suction $\dot{m}$	**Normalized Vapor injection** $\dot{m}$	**Normalized Suction** $\dot{m}$	**Normalized Vapor injection** $\dot{m}$
1	1	1	1	1
1.1	1.003	1.003	1.006	0.956
1.2	1.005	1.006	1.010	0.919
1.3	1.007	1.007	1.014	0.889
1.4	1.008	1.008	1.017	0.863
1.5	1.010	1.010	1.020	0.839

Figure 4 (b) shows the effect of condenser air flow rate at 75% load condition (300.65 K ambient temperature). It should be noted that two things were different at 75% load condition from 100% load simulation.

1) An addition of 1000 W heat was applied to the injection pipe, and was accounted for in the COP evaluation. This addition was necessary because, when the ambient temperature decreased, the approach temperature in the economizer could no longer lead to superheated vapor injection. In Figure 5 (b), we compared the 100% and 75% load P-h diagrams, at a normalized flow rate of 1. The reduced ambient temperature significantly lowered the condensing temperature. However, the injection pressure was not lowered as significantly. As a result, the approach temperature in the economizer was decreased and the injection stream in the economizer could not be heated to superheated vapor by the subcooled liquid from the condenser. As shown in the figure, the quality at J6 (inlet of the injection pipe) is roughly 0.9 or less.
2) The convergence criterion was injection SH = 1 K, instead of a fixed vapor injection ratio. Because of this, the vapor injection mass flow rate decreased with an increasing flow rate (as shown in Table 5).

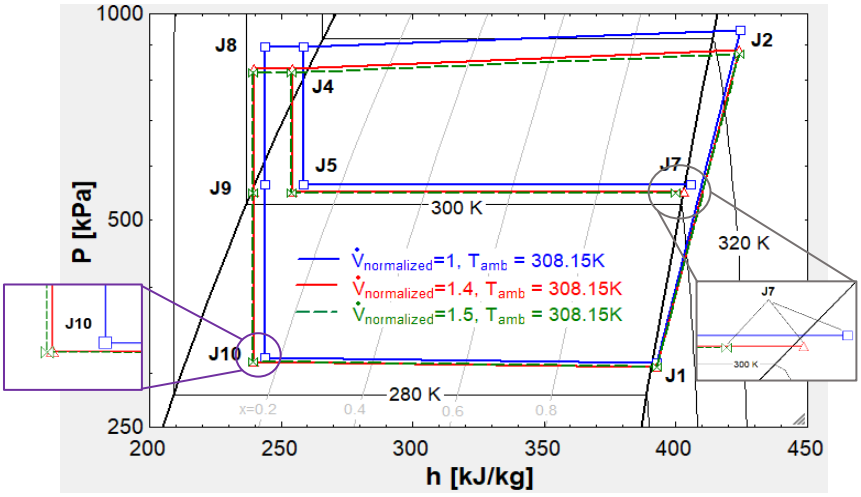

(a)

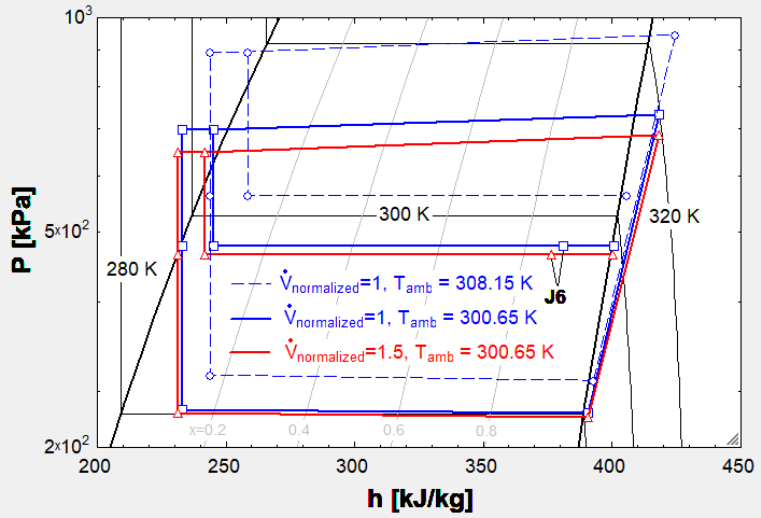

(b)

Figure 5: P-h diagrams at different condenser air flow rates and ambient temperatures

As the flow rate increases, the system capacity increases monotonically. This trend is similar to the 100% load. Figure 5 (b) shows the P-h diagram of 75% load condition at the minimum and maximum flow rate. Due to the heat addition, the injection point would remain the superheated state at all flow rates. Thus, the power consumption did not undergo accelerated increase as in 100% load. While the system COP excluding the fan power consumption increases monotonically, the COP that considers the fan power reaches the maximum when normalized flow rate is 1.2. At this optimum flow rate, the COP improvement (considering fan power) was less than 0.5%.

3.3 Effect of discharge pipe pressure drop

The effect of discharge pipe pressure drop on the system performance was very insignificant. Figure 6 shows the P-h diagram with two pressure drops (one minimum and one maximum). As shown in the figure, higher pressure drop in the discharge pipe led to a higher discharge pressure (J2), but did not affect the states at other points. Table 6 shows that higher discharge pipe pressure drop led to slightly decreased COP, capacity, power, and mass flow rates.

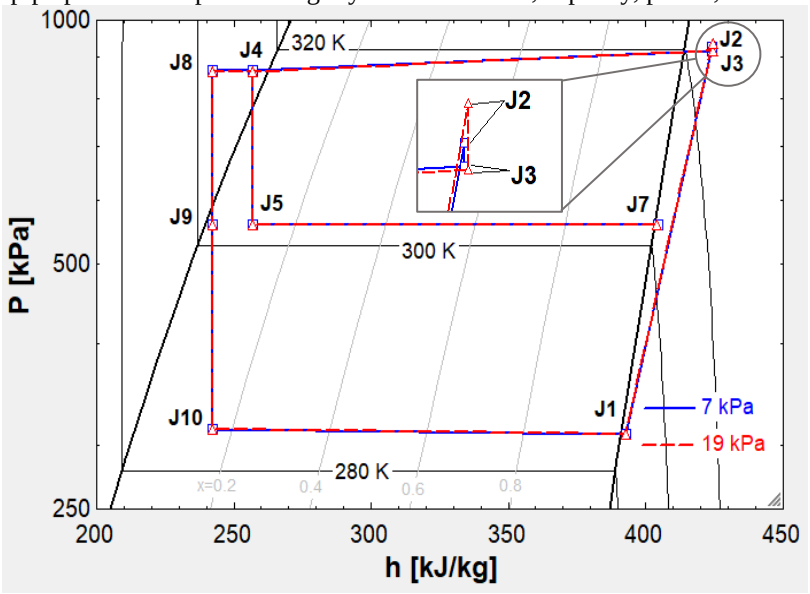

Figure 6: P-h diagrams with different discharge pipe pressure drops

Table 6: Effect of discharge pipe pressure drop on system performance and mass flow rates

Discharge pipe ΔP (kPa)	COP	Q	W	Suction $\dot{m}$	Discharge $\dot{m}$

7	-	-	-	-	-
13	-0.07%	-0.16%	-0.09%	-0.18%	-0.18%
19	-0.11%	-0.30%	-0.19%	-0.35%	-0.35%

4. CONCLUSIONS

This study presents a numerical investigation of a two-stage vapor compression system with simultaneous vapor and liquid injection. The 100% and 75% load conditions (AHRI 340/360) were investigated. We studied the effect of three variables on the system performance: vapor injection ratio, condenser air flow rate, and pressure drop in the discharge pipe. The conclusions are as follows.

(1) Effect of vapor injection ratio (R_{vi})

- As R_{vi} increases, the tradeoff in the system performance is an enhanced subcooling effect (thus larger unit refrigeration capacity) and a decreased suction mass flow rate.
- The maximum COP occurred when R_{vi} = 0.1. This conclusion is obtained assuming constant economizer effectiveness.

(2) Effect of condenser flow rate ($\dot{V}_{air}$)

- As $\dot{V}_{air}$ increases, both the system capacity and the power consumption increase. There exists an optimum $\dot{V}_{air}$ in terms of COP at both 100% and 75% load conditions.
- At 75% load condition, steady-state solution was found only with heat addition into the injection pipe. At this part load condition, the COP improvement at the optimum $\dot{V}_{air}$ was marginally less than 0.5%. This indicates that in part-load condition, vapor injection does not yield as much benefit as it does under full load condition. Optimal control strategies should be investigated to disable and enable the vapor injection during system capacity modulation.

(3) Effect of discharge pipe pressure drop

- Higher pressure drop in the discharge pipe leads to higher discharge pressure of the compressor. On the system level, it shows small impact on the overall performance in 100% load condition. However, it may have more significant effect on system performance in other test conditions.

NOMENCLATURE

h	enthalpy	(kJ/kg)
HX	heat exchanger	(–)
$\dot{m}$	mass flow rate	(kg/s)
P	pressure	(Pa or kPa)
Q	capacity	(W)
SC	subcooling	(K)
SH	superheat	(K)
T	temperature	(K)
R_{vi}	vapor injection ratio	(–)
R_{li}	motor cooling liquid injection ratio	(–)
$\hat{\dot{V}}$	normalized volumetric flow rate	(–)
$\dot{V}$	volumetric flow rate	(m^3/s)
ΔP	pressure drop	(Pa)
W	power consumption	(Pa)

Subscript

amb	ambient
comp	compressor
db	dry bulb
eco	economizer
wb	wet bulb
valv	expansion valve

REFERENCES

AHRI. (2019). *Performance Rating of Commercial and Industrial Unitary Air-Conditioning Condensing Units.* Arlington.

Aikins, K., Lee, S.-h., & Choi, J. (2013). Technology Review of Two-Stage Vapor Compression Heat Pump System. *International Journal of Air-Conditioning and Refrigeration, 21*(03), 1330002.

Dennis, J., & Schnabel, R. (1996). *Numerical methods for unconstrained optimization and nonlinear equations.* SIAM.

Heo, J., Jeong, M., Baek, C., & Kim, Y. (2011). Comparison of the heating performance of air-source heat pumps using various types of refrigerant injection. *International Journal of Refrigeration, 34*(2), 444-453.

Jiang, S., Wang, S., Jin, X., & Yu, Y. (2016). The role of optimum intermediate pressure in the design of two-stage vapor compression systems: A further investigation. *International Journal of Refrigeration, 70*, 57-70.

Jiang, S., Wang, S., Jin, X., & Zhang, T. (2015). A general model for two-stage vapor compression heat pump systems. *International Journal of Refrigeration, 51*, 88-102.

Qi, H., Liu, F., & Yu, J. (2017). Performance analysis of a novel hybrid vapor injection cycle with subcooler and flash tank for air-source heat pumps. *International Journal of Refrigeration, 74*, 540-549.

Torrella, E., Larumbe, J., Cabello, R., Llopis, R., & Sanchez, D. (2011). A general methodology for energy comparison of intermediate configurations in two-stage vapour compression refrigeration systems. *Energy, 36*(7), 4119-4124.

ACKNOWLEDGEMENT

This work was supported by the Modeling and Optimization Consortium (MOC) at the University of Maryland. The authors also acknowledge Danfoss A/S for contributing to the system model development.